

The Design and Performance of the Ocean Radiometer for Carbon Assessment (ORCA)

Mark E. Wilson
Optics Branch
NASA Goddard Space Flight Center
Greenbelt, MD 20771

Abstract- A design concept for an advanced ocean color radiometer, the Ocean Radiometer for Carbon Assessment (ORCA) has been built at NASA Goddard Space Flight Center (GSFC) and tested at the National Institute of Standards and technology (NIST). The presentation will review the ORCA performance requirements, the basic design concept, and performance test results to date.

All these requirements affect the sensor design in one way or another. The lunar calibration is a mission requirement in that the mission must support whatever maneuvers or sensor positioning on the spacecraft to allow monthly views of the moon at a constant phase angle, i.e. 7° like SeaWiFS [6].

I. Introduction

Over the last 3 years, a prototype version of ORCA was built and tested to determine if the design meets the proposed requirements for the ACE, or PreACE (PACE) mission ocean radiometer. The design concept was presented at last year's ESTO conference¹. This paper will present the results of this testing.

II. ACE Ocean Measurement Requirements

Table I shows the preliminary wavelength bands, the values for L_{typ} and L_{max} , and minimum SNR values at those wavelengths. The L_{max} values are the saturation radiances. The ACE requirement is that no bands saturate. The ORCA SNR-model values are for a 650 km altitude, which was the initial ACE altitude and is the basis for the ORCA prototype design. The ORCA modeled SNRs are based on measured component reflectances, transmittances, and vendor quotes on detector performance. The primary performance and design requirements are listed below:

1. A minimum of 26 hyperspectral bands (Table 1)
2. Spectral resolution: 5 nm (345-775 nm)
3. Sensor polarization sensitivity: $< 1.0\%$
4. Global coverage every two days
5. Spatial resolution: 1 km
6. Tilt (sun glint avoidance): 20° fore/aft
7. No multispectral band saturation
8. Stability: $< 0.1\%$ knowledge – mission duration, $< 0.1\%$ over one month – prelaunch demonstration
9. Prelaunch calibration uncertainty $< 2\%$ maximum, 0.5% goal.
10. Accommodate lunar calibration

λ	$\nabla\lambda$	L_{typ}	L_{max}	ACE SNR-specification	ORCA SNR-model
350	15	7.46	35.6	300	2020
360	15	7.22	37.6	1000	2225
385	15	6.11	38.1	1000	2370
412	15	7.86	60.2	1000	3156
425	15	6.95	58.5	1000	3006
443	15	7.02	66.4	1000	3048
460	15	6.83	72.4	1000	3062
475	15	6.19	72.2	1000	2960
490	15	5.31	68.6	1000	2740
510	15	4.58	66.3	1000	2575
532	15	3.92	65.1	1000	2192
555	15	3.39	64.3	1000	2011
583	15	2.81	62.4	1000	2203
617	15	2.19	58.2	1000	2010
640	10	1.90	56.4	1000	1660
655	15	1.67	53.5	1000	1830
665	10	1.60	53.6	1000	1562
678	10	1.45	51.9	1400	1510
710	15	1.19	48.9	1000	1616
748	10	0.93	44.7	600	1305
765	40	0.83	43.0	600	2512
820	15	0.59	39.3	600	1200
865	40	0.45	33.3	600	1640
1245	20	0.088	15.8	250	415
1640	40	0.029	8.2	250	273
2135	50	0.008	2.2	100	146

Radiance units: $mW/cm^2 nm str$

Table 1. ACE ocean radiometer required multispectral bands, nominal bandwidths, typical clear weather top of the atmosphere radiances over the ocean, maximum radiances over clouds, minimum SNRs, and modeled ORCA SNRs.

III. The ORCA Prototype

The functional design of the optics is shown in Figures 1. A photograph of the hardware is in Figure 2. In this design, the collecting aperture is 90 mm in diameter. The incoming beam is focused to a slit using an off axis ellipsoidal mirror. The primary is followed in the optical path by a depolarizer consisting of two wedged pieces of magnesium fluoride with a

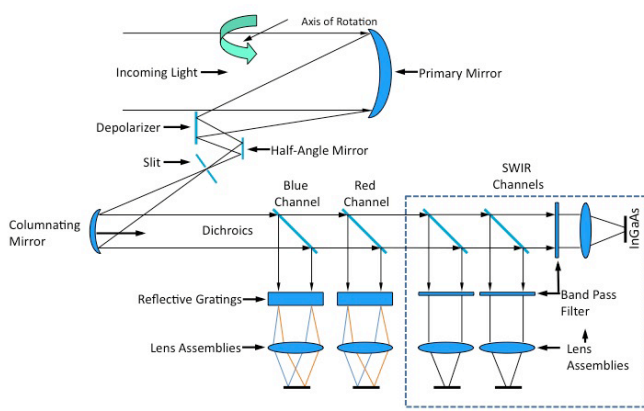


Figure 2 - Functional optical diagram

reflective coating on the backside of the second piece. The primary mirror and depolarizer are rotated as a unit. Both are surrounded by a tube, which serves to provide baffling against stray light from outside the science field of view. To “unrotate” the image and allow the light to transmit through the slit, a half angle mirror is used. This mirror must be flat and coated on both sides of the mirror.

The slit in the current implementation of ORCA is coated on both sides with a layer of carbon nanotubes, developed at NASA/GSFC. The substrate material is silicon. The slit itself is not the traditional narrow slit used frequently in astronomy – the narrow width of the slit is about 600 microns wide.

After the slit, the beam is collimated. It gets split in different spectral bands by using dichroic beamsplitters; the light from 350-565 nm is referred to as the “blue channel”, the light between 575 and 885 nm is the “red channel”, and light between 1245 and 2130 nm is the SWIR channel.

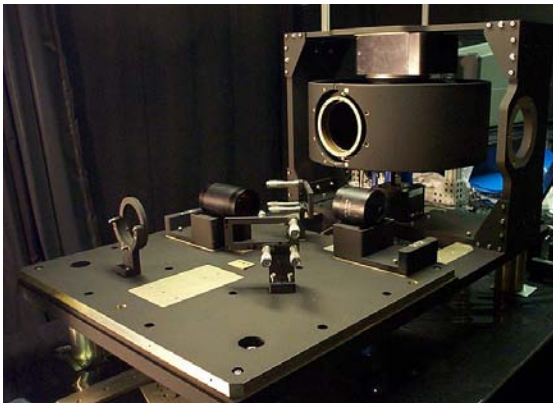


Figure 1 - The ORCA prototype undergoing fabrication and alignment in the ORCA calibration facility at GSFC.

Testing at NIST concentrated on basic optical design verification: spectral resolution, spatial imaging, and issues of stray and scattered light. No dynamic tests were conducted with the telescope assembly rotating because there was no method available to synchronize the detector readout with the mechanism motion – this will be performed during a second IIP awarded to ORCA. For the current testing, all images taken were static.

To determine spectral dispersion, each of the two CCD bands was tested using the NIST CIRCUS lasers, which have a residual bandwidth of ~0.1 nm. Both bands were covered over the full wavelength range plus some wavelengths outside the band. Measurements were made every few nanometers, typically around 3 nm. The light from the laser was fed through a fiber which was located at the focus position of an off axis parabola, which collimate the light entering the instrument. At the detector of the instrument, calculations of the pixel position versus wavelength were made and a calculation of the dispersion was made. This was done only for light at the center of the slit

A. Spectral Dispersion

Both the red channel (shown in Figure 3a) and blue channel (Figure 3b) dispersion is quite linear. The slopes of the lines should give a result of 5 nm/superpixel. For the red channel, it can be seen that the result is 4.9 nm/superpixel, and for the blue channel the result is 5.02 nm/superpixel. The implication is that the groove density of the grating and focal length of the focusing lens are correct for the blue channel, and close to correct for the red channel, with the groove density being 2.5% too dispersive.

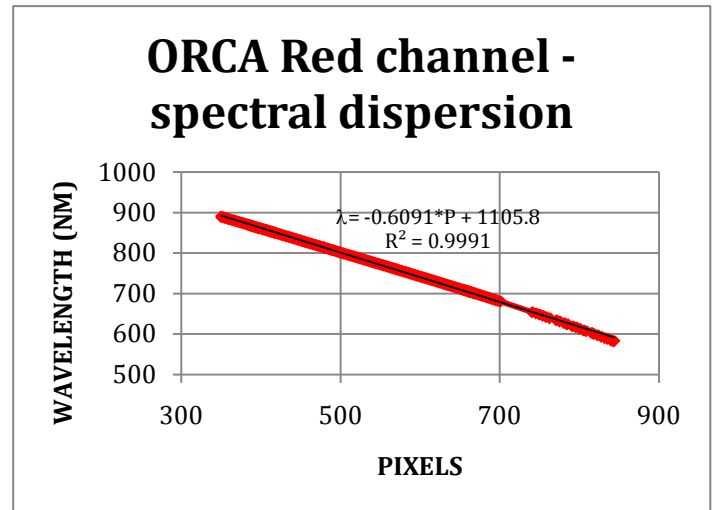


Figure 3 Red Channel spectral dispersion

IV. Testing Results

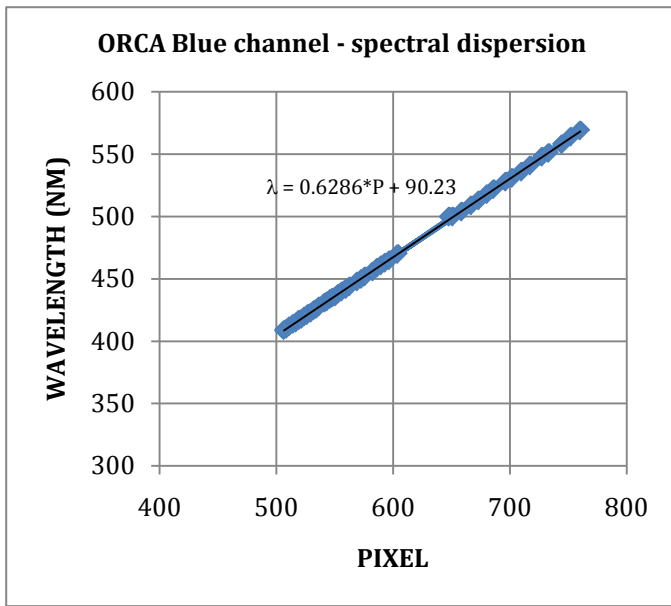


Figure 4 Blue Channel Dispersion

B. Spectral Slit Width

The spectral resolution, of course, is determined by not just the dispersion but the width of the slit images. To do this measurement, an integrating sphere was used – the laser was connected by fiber to the sphere, then the sphere was placed in front of ORCA. The results are shown in Figure 5 for the red channel, Fig. 6 for the blue channel. These figures indicate that the red channel has slit widths that exceed the desired width. This is due to the anamorphic magnification inherent in a grating system. With an average slit width of 10 pixels, this gives a spectral resolution of 7.6 nm/superpixel (goal is 5). Adjusting the design to achieve the desired slit width poses no problems.

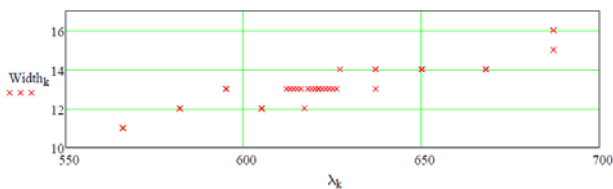


Figure 5 Red channel slit width as function of wavelength

The blue channel gives a result of 9 pixels for the slit width, giving a resolution of 6 nm/superpixel. This difference (6 vs 5) is to a large extent due to the way the slit width was defined during the optical design process.

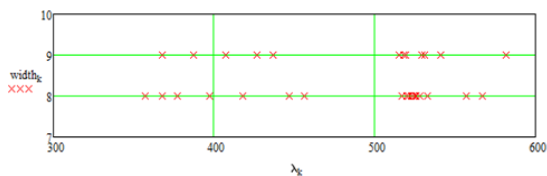
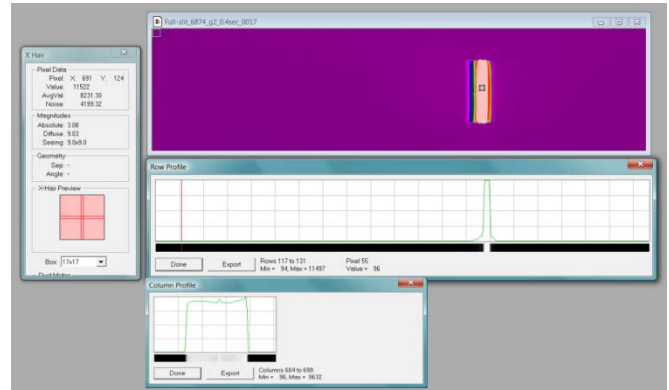


Figure 6 Blue channel slit width as function of slit width

A more specific example is shown in Figure 7.



The calculation of spectral resolution results in 7.9 nm per superpixel for the red channel, 6.0 nm per superpixel for the blue channel. The goal is 5 nm/superpixel

C. Imaging

There were two concerns with the imaging characteristics of the instrument – in the spectral direction, image blur could reduce the spectral resolution, and in the spatial direction the blur would degrade the spatial resolution. The goal of the optical design was to achieve an encircled energy >60% in 2 physical pixels, particularly at the edges of the IFOV (i.e. a superpixel).

The full width half maximum of individual PSFs over the full array for both the red and blue channels are shown in Figures 8 (red) and 9 (blue). These results show that the image quality of the red channel is about 2 pixels diameter for wavelengths > 640 nm, increasing to 2.5 pixels at the short end of the band. For the blue channel, the FWHM of the blurs are < 2 pixels for all wavelengths below 520 nm, and increase to 2.5 pixels. Some of this increase may be due to a wavelength broadening of the source at those wavelengths. One note is that these results include the several images that are created when the beam travels through the birefringent depolarizer.

Encircled energy calculations indicate that the 80% levels are reached in diameters ranging from 5-5.5 pixels, so that the full images are rather large. This is not thought to be a problem.

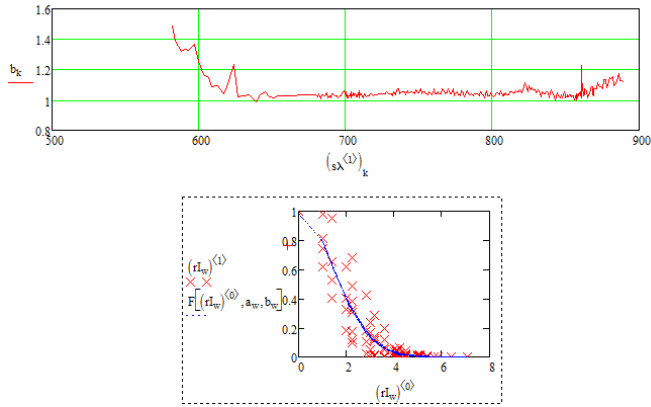


Figure 8 - Image blur size (radius, in pixels) as a function of wavelength for Red channel; also shown is fit to a Gaussian

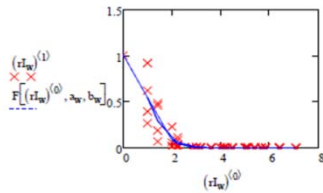


Figure 9 Image blur size (radius, in pixels) as a function of wavelength for Red channel; also shown is fit to a Gaussian

D. Polarization Sensitivity

To measure the polarization sensitivity, a broad band source supplied by NIST was used. This source covered the full wavelength ranges for both the red and blue channels. The light from this source was fed into an integrating sphere, then through a large MOXTEK polarizer placed between the sphere and ORCA. The residual polarization of light coming out of the sphere was measured and was so small as to be discounted.

The polarization sensitivity was performed for different orientations of the telescope and with both sides of the HAM. There were 3 rotation angles tested, 0, 20, and 50 deg from nadir. The results of the tests are shown in Figures 10&11. From these results, it is evident that the polarization sensitivity is < 1% for the large portion of the wavelength bands in each channel. It is seen that the wavelengths that exceed 1% are at the long end of the blue channel and the short end of the red channel. It should be possible to correct this to meet specifications in the future. It should be mentioned that using TDI (Time Delay Integration) helps improve the polarization response of the instrument, by averaging pixels instead of looking at every individual pixel.

Blue Side A and B telescope polarization sensitivity for the following telescope angles = 0° (nadir), 50° and 20° from nadir.

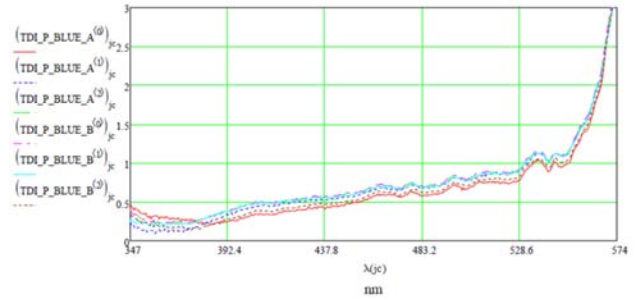


Figure 10 Blue channel polarization sensitivity

Red Side A and B telescope polarization sensitivity for the following telescope angles = 0° (nadir), 50° and 20° from nadir.

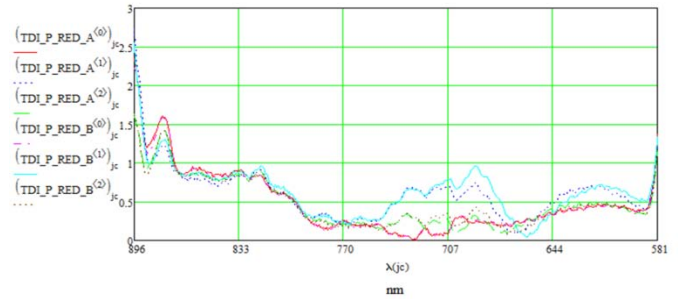


Figure 11 Red channel polarization sensitivity

E. Stray Light and Scattered Light

To minimize the effect of stray light (i.e. light from outside the field of view and unwanted grating orders), it was decided to put a baffle tube in front of the primary mirror and to make the aperture stop located internal to the instrument optics. Currently it is located after the collimator, at the relayed image of the primary mirror. The use of an internal stop allows the instrument to view only the HAM, not the surrounding structure, so the instrument response would not change during telescope rotation.

Standard stray light suppression techniques were used, such as painting the structure with Z306. It was also decided that, as long as a suitable adherence material could be found which blocked SWIR light from transmitting through the slit substrate, carbon nanotubes would be used on both sides of the slit.

The front cover of the instrument also provides stray light suppression. The rotating telescope is located inside of a (nonmoving) shield which has an opening wide enough to allow a +/-58 deg field of regard on the Earth. All the materials are coated with Z306.

Prior to testing, we were aware of one source of stray light – the front surface of the depolarizer generates a reflected beam, about 3% of the incoming beam intensity. The solution would

be to put a wedge on the front surface of the depolarizer as was done in SeaWiFS, to steer this ghost reflection onto the main science path – this way it can be calibrated out because it is always present. Another possible method, being studied in an SBIR right now, is to put a diffractive structure (i.e. a moth’s eye coating) on the front of the depolarizer.

During testing, other specific stray light tests were performed. Images were examined to see if there were light levels above the ambient noise of the detector. After system alignment, there were no cases where spurious light was evident. During the alignment process, it was clear when outside sources would reach the detectors.

A measure of infield scattered light was performed by placing the input beam just outside of the slit and measuring the amount of light which still gets through the slit. Scattered light was detected, but is attributed in large part to continuation on the optical surfaces and surface roughness.

The rms surface roughness values for the primary mirror was measured at roughly 10 Angstroms, and the same will be done for spares of the collimator and HAM. The goal is to build up a high fidelity model, predict the results, and see how close they match the data. This is an ongoing topic of discussion by the ORCA team. There are also ghost contributions from the diffraction gratings. Figure 11 shows some ghosts; they are down to about 10^{-3} of the peak intensity

F. Summary

To date, a prototype level of ORCA has been assembled, aligned, and tested. The initial results for spectral resolution are very close to meeting spec for the blue channel, but show that a modification (currently underway) is needed for the red channel. Results for polarization sensitivity also meet spec over a large portion of the bandpass, but a method of keeping all the values below 1% needs to be developed. Off axis stray light rejection looks good, but more specific tests will need to be done. Scattered light is thought to be the item of largest concern in the optics area. Further refinements in the design, e.g., depolarizer design, are underway.

1. References

- [1] Charles R. McClain, *The Ocean Radiometer for Carbon Assessment (ORCA)*, NASA Goddard Space Flight Center, Greenbelt, MD, 2010.

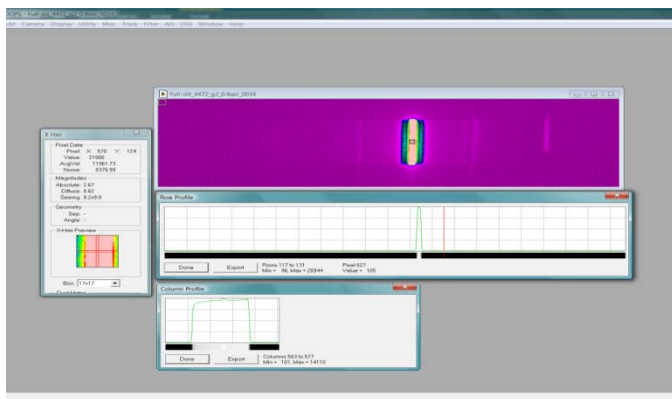


Figure 12 Ghosts seen in blue channel

We are also working on a method of taking the measured data, combining it with the known source and detector data, to calculate the optical transmission as a function of wavelength. At this point in time there is no reason to believe there is any serious problems with the values calculated from component measurements.